available at www.sciencedirect.com

ScienceDirect

journal homepage: www.elsevier.com/locate/biochempharm

Induction of G_2/M arrest, endoreduplication, and apoptosis by actin depolymerization agent pextenotoxin-2 in human leukemia cells, involving activation of ERK and JNK

Dong-Oh Moon [a], *Mun-Ock Kim* [b], *Sang-Hyuck Kang* [a], *Kyeong-Jun Lee* [a], *Moon-Soo Heo* [a], *Kwang-Sik Choi* [a], *Yung Hyun Choi* [c], *Gi-Young Kim* [a,*]

[a] *Faculty of Applied Marine Science, Cheju National University, Jeju Special Self-Governing Province 690-756, South Korea*
[b] *Department of Microbiology, College of Natural Sciences, Pusan National University, Busan 609-735, South Korea*
[c] *Department of Biochemistry, Dongeui University College of Oriental Medicine, Busan 614-052, South Korea*

ARTICLE INFO

Article history:
Received 6 February 2008
Accepted 5 May 2008

Keywords:
Pectenotoxin-2
G_2/M phase arrest
Endoreduplication
Apoptosis
Actin depolymerization

ABSTRACT

Pectenotoxin-2 (PTX-2) is a natural compound from marine sponges and has been known to inhibit cytokinesis through the depolymerization of actin filaments. To investigate the role of actin dysfunction by PTX-2 in human leukemia cells, we analyzed the effect of PTX-2 on the cell cycle and apoptosis. Cell cycle analysis showed that the depolymerization of actin with PTX-2 induces G_2/M phase arrest at 12 h and endoreduplication at 24 h. Analysis of the cell cycle regulatory proteins demonstrated that PTX-2 increases phosphorylation of cdc25c and decreases the protein levels of cdc2 and cyclin B1. The M phase specific marker protein, phospho-histone 3, was also increased by PTX-2. Furthermore, p21 and CDK2, which are associated with the induction of endoreduplication, were also upregulated. PTX-2 also inhibited the growth of leukemia cells and caused a marked increase in apoptosis, as characterized by annexin-V^+ cells and caspase-3 activity. Interestingly, we found that induction of G_2/M phase arrest, endoreduplication, and apoptosis by PTX-2 is regulated by the extracellular signal-regulated kinase (ERK) and c-jun N-terminal kinase (JNK) pathway. Inhibitors of ERK and JNK more increased the phosphorylation of cdc25c expression at G_2/M arrest stages, and decreased p21 and CDK2 expression at endoreduplication stages and Bax expression at apoptotic stages in the presence of PTX-2. These molecular mechanisms provide that PTX-2 induces G_2/M phase arrest, endoreduplication, and apoptosis through the ERK and JNK signal pathway *via* actin depolymerization.

1. Introduction

Actin is one of the most abundant and common cytoskeletal proteins for cell growth, motility, signaling, and maintenance of cell shape [1,2]. It has been recognized that control of the actin cytoskeleton must be coordinated with control of cell cycle events [3]. Cell cycle progression into G_1, S, and G_2/M phases has been shown to be controlled by actin. In the G_0/G_1 phase, actin serves as the major component of stress fiber and concentrates in a contractile ring at the end of the S phase. In the G_2/M phase, the contractile ring constricts down to the cell midbody, forming an intercellular bridge [4]. Recent studies

* *Corresponding author*. Tel.: +82 64 754 3427; fax: +82 64 756 3493.
E-mail address: immunkim@cheju.ac.kr (G.-Y. Kim).

Abbreviations: PTX-2, pectenotoxin-2; ERK, extracellular signal-regulated kinase; JNK, c-jun N-terminal kinase; MAPK, mitogen-activated protein kinase.

0006-2952/$ – see front matter © 2008 Elsevier Inc. All rights reserved.
doi:10.1016/j.bcp.2008.05.006

have investigated whether the binding and stabilizing of actin microfilaments using actin polymerization inhibitors could inhibit the growth of several tumor cell lines [5,6]. Because these cytotoxin agents have been shown to play important roles in anticancer therapy due to their ability to interfere with actin cytoskeleton dynamics, their potential utility in the treatment of cancer has been recognized [7,8]. However, the precise mechanism that induces cell growth arrest and stimulates apoptosis by actin interfering agents is unknown.

Pectenotoxins (PTXs) are polyether macrolides found in certain *Dinoflagellates*, sponges, and shellfish, and have been associated with diarrheic shellfish poisoning [9,10]. To date, 14 PTXs have been isolated and characterized, among them, PTX-2 has especially been shown to have a potently cytotoxic effect in human cancer cell lines [11]. Recent studies have also demonstrated that the anticancer effect of PTX-2 is due to disruption of the actin cytoskeleton through the inhibition of actin polymerization, whereby a complex is formed with G-actin [12,13]. However, the detailed biochemical properties of this compound on anticancer therapy have not yet been reported and there is no evidence that PTX-2 induces endoreduplication.

In the present study, our aim is to elucidate the PTX-2–induced anticancer mechanism in human leukemia cells. We found evidence that PTX-2 strongly induced G_2/M arrest, endoreduplication, and apoptosis in a time-dependent manner *via* promoting actin depolymerization. These events are coordinated with the activation of mitogen-activated protein kinases (MAPKs), and in particular extracellular-signal regulated kinase (ERK) and c-jun-N-terminal kinase (JNK). Inhibition of ERK and JNK signaling pathways by inhibitors prevented PTX-2-induced cell cycle disruption and apoptosis.

2. Materials and methods

2.1. Reagents and antibodies

PTX-2 was prepared as described previously [14] and dissolved in DMSO (vehicle control) as a stock solution at 1 mg/ml concentration, and stored in aliquots at −20 °C. Phalloidin-FITC, 3-(4,5-dimethylthiazol-2-yl)-2,5-diphenyltetrazolium bromide (MTT), 4,6-diamidino-2-phenylindole (DAPI), and propidium iodide (PI) were purchased from Sigma (St. Louis, MO) and an enhanced chemiluminescence (ECL) kit was purchased from Amersham (Arlington Heights, IL). PD98059, SB203580, and SP600125 were obtained from Calbiochem (San Diego, CA). RPMI 1640 medium was purchased from Invitrogen Corp. (Carlsbad, CA) and fetal bovine serum (FBS) was purchased from GIBCO-BRL (Gaithersburg, MD). All other chemicals not specifically cited here were purchased from Sigma.

2.2. Antibodies

Anti-cyclin B1, anti-cdc2, anti-phospho (p)-cdc25c, anti-p21, anti-CDK2, anti-caspase-3, anti-PARP, anti-Bcl-2, anti-Bax, anti-p-topoisomerase (Topo) II, and anti-Topo II were purchased from Santa Cruz Biotechnology (Santa Cruz, CA). Anti-p-histone (H) 3, anti-p-ERK, anti-ERK, anti-p-p38, anti-p38, anti-p-JNK, anti-JNK, anti-p-c-jun, anti-c-jun, anti-p-ATF-2, and anti-ATF-2 were purchased from Cell Signal (Beverly, MA). Peroxidase-labeled donkey anti-rabbit and sheep anti-mouse immunoglobulin were purchased from Koma Biotechnology (Seoul, South Korea).

2.3. Cell lines and culture

Human leukemia U937, HL60, THP-1, and K562 cells, human breast cancer cell MDA-MB-231, and human hepatoma cell Hep3B were obtained from the American Type Culture Collection (Rockville, MD). Cells were cultured at 37 °C in a 5% CO_2 humidified incubator, and maintained in an RPMI 1640 culture medium containing 10% heat-inactivated FBS. Cells were seeded at 5×10^4 cells/ml and treated with PTX-2 at the indicated times. Cell viability and proliferation were determined by MTT assay and trypan blue exclusion assay, respectively.

2.4. Binding of FITC-phalloidin to actin polymer

For determination of the amount of F-actin, cells were stained with phalloidin-FITC at a concentration of 0.05 mg/ml. Cells were then analyzed using a FACSCalibur flow cytometer (Becton Dickenson; San Jose, CA).

2.5. Nuclear staining

After treatment with PTX-2, cells were harvested, washed in ice-cold PBS, fixed with 3.7% paraformaldehyde and then permeabilized with 0.5% Triton-X 100. Fixed cells were washed with PBS and nuclei were stained with DAPI solution. Nuclear morphology was evaluated by fluorescence microscopy.

2.6. Cell cycle analysis

The cell cycle was analyzed using a flow cytometer of PI-stained cells. Cells (1×10^6) were fixed in 70% ethanol overnight at 4 °C. The cells were washed in phosphate-buffered saline with 0.1% BSA. Cells were incubated with 1 U/ml of RNase A (DNase free) and 10 μg/ml of PI overnight at room temperature in the dark. Cells were analyzed using a FACSCalibur flow cytometer and CellQuest software (Becton Dickinson) was used to determine the relative DNA content based on the presence of a red fluorescence.

2.7. Western blotting

The total cell extracts were prepared using PRO-PREP protein extraction solution (iNtRON Biotechnology; Seoul, South Korea). The preparation of nuclear extracts was carried out using the NE-PER nuclear extraction reagents (Pierce; Rockford, IL). Protein concentration was quantified using the Bio-Rad detergent-compatible protein assay reagent (Bio-Rad Laboratories; Hercules, CA). Fifty micrograms of the total cell extracts were separated on 10% polyacrylamide gels and then transferred to nitrocellulose membranes using standard procedures. The membranes were blocked in 5% powdered milk in TBST and incubated with primary antibodies overnight at 4 °C. Blots were washed three times for 10 min in TBST and probed with mouse or rabbit secondary antibodies for 1 h. The membranes were washed three times for 10 min in TBST and then developed using the ECL reagent.

2.8. Topo II activity in nuclear extracts

The Topo II activity in nuclear extracts was assayed using an assay kit (TopoGen; Columbus, OH) based upon the decatenation of kinetoplast DNA (kDNA). After incubation for 40 min at 37 °C, the samples were loaded onto 1% agarose gels and subjected to electrophoresis for 2.5 h at 100 V.

2.9. Tubulin polymerization in vitro assay

Fifty microlitres of 5 mg/ml pure tubulin (Cytoskeleton; Denver, CO) were brought to a steady state in G-PEM buffer (100 mM PIPES (pH 6.9), 1 mM EGTA, 1 mM $MgCl_2$, and 1 mM GTP) plus 10% glycerol in a 96-well plate (0.33 cm^2/well), by incubation at 37 °C for 30 min. The effects on polymerization/depolymerization were quantified by measuring the absorbance at 340 nm (A_{340}) over time.

2.10. In vitro caspase-3 activity assay

The activity of caspase-like protease was measured using a caspase activation kit according to the manufacturer's protocol. This assay is based on spectrophotometric detection of the color reporter molecule *p*-nitroanaline (*p*NA), which is linked to the end of the caspase-specific substrate. The cleavage of the peptide by the caspase releases the chromophore *p*NA, which can be quantified spectrophotometrically at a wavelength of 405 nm. Ac-DEVD-*p*NA is used as the substrate.

2.11. Annexin-V staining

U937 cells at 5×10^4 cells/ml were treated with PTX-2 for 72 h and the cells were harvested in binding buffer, supplemented with 5 μl of annexin-V (PharMingen; San Diego, CA) and incubated for 30 min at room temperature in the dark. Flow cytometric analysis was performed as described previously.

2.12. Statistical analysis

All data were derived from at least three independent experiments. The images were visualized with Chemi-Smart 2000 (Vilber Lourmat, Marine; Cedex, France). Images were captured using Chemi-Capt (Vilber Lourmat) and transported into Photoshop. Scion Imaging software (http://www.scioncorp.com) was used to quantify the Western blots. Statistical analyses were conducted using SigmaPlot software, and values were presented as mean ± S.D. Significant differences between the groups were determined using the unpaired Student's *t*-test. A value of $^*p < 0.05$ was accepted as an indication of statistical significance.

3. Results

3.1. Actin depolymerization by PTX-2 inhibits cell proliferation

It has been reported that PTX-2 is known to be a powerful inhibitor of cytokinesis through inhibition of actin polymerization [11–13]. However, the effects of PTX-2 in human cancer cells have not been determined. Therefore, we first investigated the effects of PTX-2 on the viability and proliferation of leukemia cells by MTT assay and cell counting assay, respectively. As shown in Fig. 1A and B, treatment with more than 6 ng/ml of PTX-2 for 72 h decreased cell viability and proliferation in U937, THP-1, HL-60, and K562 cells. Furthermore, we examined the effect of PTX-2 on the binding of phalloidin-FITC to actin. This binding assay is based on a titration of polymerized actin against a constant concentration of phalloidin-FITC by monitoring the fluorescence intensity of the fluorophore [15]. As shown in Fig. 1C, PTX-2 treatment for 1 h decreased the fluorescence intensity of phalloidin-FITC in a dose-dependent manner in human leukemia U937 cells. These results indicate that PTX-2 causes a decrease in cell viability and proliferation through the depolymerization of actin.

3.2. PTX-2 induces enlarged cells through the inhibition of cytokinesis

In order to investigate whether PTX-2 inhibits cytokinesis *via* actin dysfunction in human leukemia cells, we stimulated in four leukemia cells with 10 ng/ml of PTX-2 for 72 h. To analyze the effect of PTX-2 on mitotic cell division in the leukemia cells, the cells were stained with DAPI to visualize DNA. As shown in Fig. 2A, the leukemia cells failed to complete mitotic division and remained in the one-cell stage, but with multiple nuclei. It is well known that maintenance of constant cell size during cellular proliferation must be coordinated with the rate of cell division. To next investigate whether the failure of mitotic cell division as caused by PTX-2 induces an increase in cell size, we observed and quantified cell size using a light microscope and flow cytometer. As shown in Fig. 2B and C, 10 ng/ml of PTX-2 treatment for 72 h contributed to increase in cell size. These results indicate, in accordance with previous studies, that PTX-2 prevents cell division by actin disruption and induces oversized cells.

3.3. Topo II activity and microtubulin are not involved in PTX-2-induced G_2/M phase arrest and endoreduplication

Recent studies have demonstrated that the reduction of Topo II activity induces endoreduplication in cancer cells [16,17]. In order to determine whether PTX-2-induced endoreduplication is associated with Topo II activity, we carried out an *in vitro* Topo II catalytic assay. As can be seen in Fig. 3A and B, treatment with PTX-2 for 24 h partially increased Topo II activity in U937 leukemia cells. PTX-2 also induced phosphorylation of Topo II in the nucleus of U937 cells (Fig. 3C). On the basis of these results, since endoreduplication is known to be linked with the inhibition of Topo II activity, this effect of PTX-2 is not associated with Topo II.

Microtubules play important functions in cell replication and division, the maintenance of cell shape, and cellular movement. Since the disruption of dynamics of microtubule polymerization has been known to induce endoreduplication [18], we reasoned that the microtubule network might itself be a target of PTX-2-induced endoreduplication. To address this question, we examined the direct effect of PTX-2 on tubulin polymerization/depolymerization using *in vitro* tubulin poly-

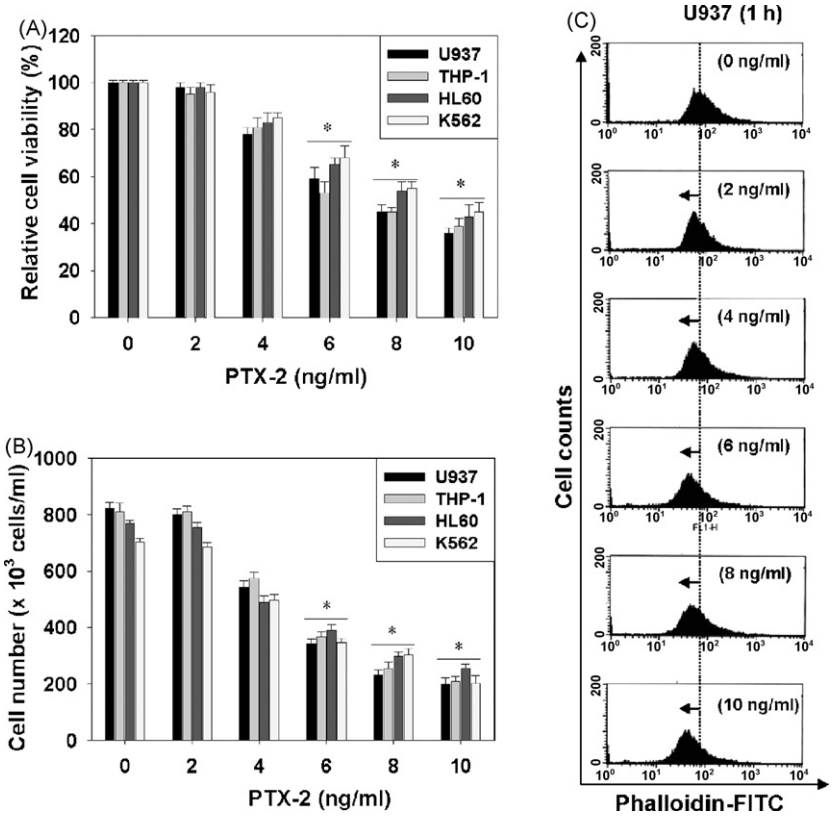

Fig. 1 – Actin depolymerization agent, PTX-2, decreases cell viability and cell proliferation in human leukemia cells. Cells were seeded at 5×10^4 cells/ml and incubated for 12 h. The cells were treated with the indicated concentrations of PTX-2 for 72 h. Cell viability (A) and cell proliferation (B) were determined by MTT assays and hemocytometer counts of trypan blue-excluding cells, respectively. Each point represents the mean ± S.D. of three independent experiments. The significance was determined using Student's *t*-test (*$p < 0.05$ vs. vehicle control). (C) U937 cells exposed to the indicated concentrations of PTX-2 for 1 h, stained with phalloidin-FITC, and then analyzed using flow cytometric analysis.

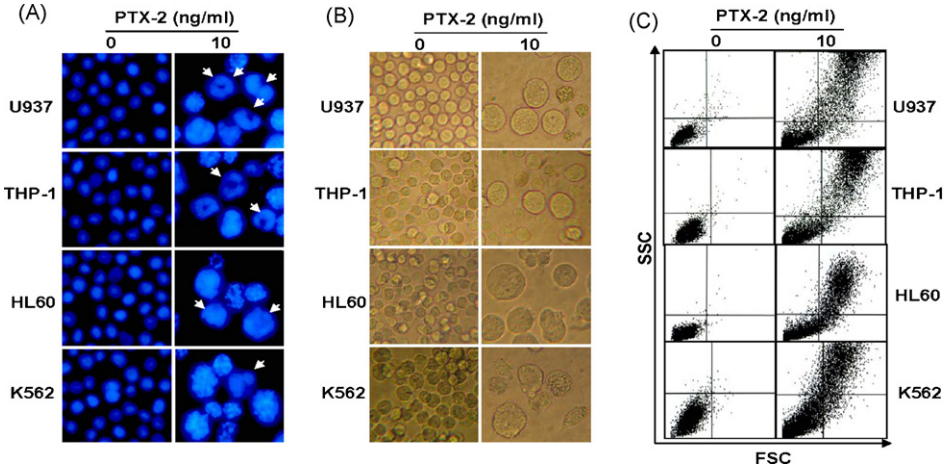

Fig. 2 – PTX-2 inhibits mitosis and induces large cell sizes. Cells were seeded at 5×10^4 cells/ml and then treated with PTX-2 (10 ng/ml) for 72 h. (A) The cells were fixed and stained with DAPI to visualize DNA. Cells were analyzed by fluorescence microscopy (×400). White arrows represent the multi-nucleus. (B) The morphology of cells treated with or without PTX-2 was examined under light microscopy (×400). (C) Cell size (FSC) and intracellular granules (SSC) were detected by flow cytometric analysis.

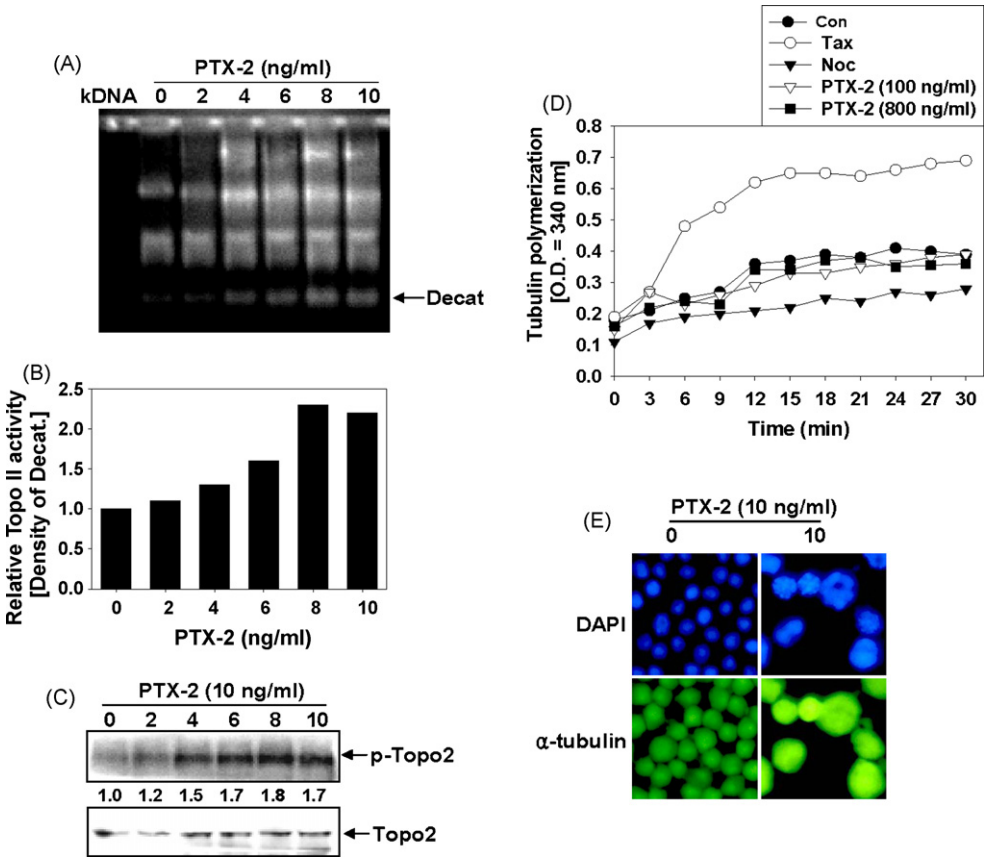

Fig. 3 – Topo II and tubulin are not targets of PTX-2–induced endoreduplication. (A) Nuclear extracts of U937 were obtained 24 h after PTX-2 treatment. The ability of Topo II to decatenate catenated kinetoplast DNA after incubation with nuclear extracts was assayed by DNA gel electrophoresis. (B) The respective densitometric profiles of Topo II ability are shown. (C) The expression of Topo II and p-Topo II were detected by Western blotting using nuclear extracts from U937 cells. (D) Effects of PTX-2 on *in vitro* microtubulin polymerization. Microtubule associated protein-rich tubulin (1 mg/ml) was incubated at 37 °C for 0–30 min and treated with the indicated concentrations of PTX-2, 3 μM nocodazole (Noc) and 3 μM paclitaxel (Tax). A_{340} values were recorded once per 3 min. (E) Microtubule immunofluorescence of U937 cells treated for 72 h with PTX-2 (10 ng/ml). Cells were fixed, permeabilized, and stained with the anti-α-tubulin monoclonal antibody. The monoclonal antibody was detected using an antimouse secondary antibody conjugated with Alexa Fluor® 488 and then stained with DAPI solution. Stained-α-tubulin and nuclei were then observed under a fluorescent microscope (×400).

merization assays. As expected, the addition of paclitaxel (3 μM), which is known to be a tubulin polymerization agent, caused an increase in tubulin polymerization, in contrast, 3 μM of nocodazol caused a decrease in tubulin polymerization. PTX-2 (100 and 800 ng/ml) did not change tubulin polymerization *in vitro* (Fig. 3D). However, in immunofluorescence analysis, it seemed that PTX-2~ promotes an intensity of staining in α-tubulin (Fig. 3E). These contradictory data might result from the induction of giant cell sizes by PTX-2, because oversized cells could contain large amounts of α-tubulin. These results mean that microtubulin is not a target for PTX-2.

3.4. *PTX-2 induces G_2/M phase arrest and endoreduplication in leukemia cells*

PTX-2 has been known to inhibit tumor cell growth through the induction of apoptosis [11]. However, the mechanism by which PTX-2 acts on cell cycle distribution is largely unknown. Fig. 4A shows typical histograms of cell cycle distribution in four leukemia cells in the presence or absence of 10 ng/ml of PTX-2. Treatment with PTX-2 (10 ng/ml) strongly induced G_2/M phase arrest at 12 h. A large number of arrested cells appeared at 12 h in the G_2/M phase underwent endoreduplication at 24 h. Moreover, the sub-G_1 population, which indicates apoptotic cell death, increased very slightly at 24 h in the presence of PTX-2.

To characterize the G_2/M phase arrest more clearly, the proteins expression changes were examined that have been known to control the G_2/M cell cycle phase transition in U937 cells. In comparison to control cells, cells treated with PTX-2 exhibited a dose-dependent decrease in the levels of cyclin B1 and cdc2 (Fig. 4B), which is consistent with the role of these proteins in the regulation of the G_2/M phase transition. The function of cdc25c is negatively regulated by phosphorylation at Ser-216, which creates a binding site for

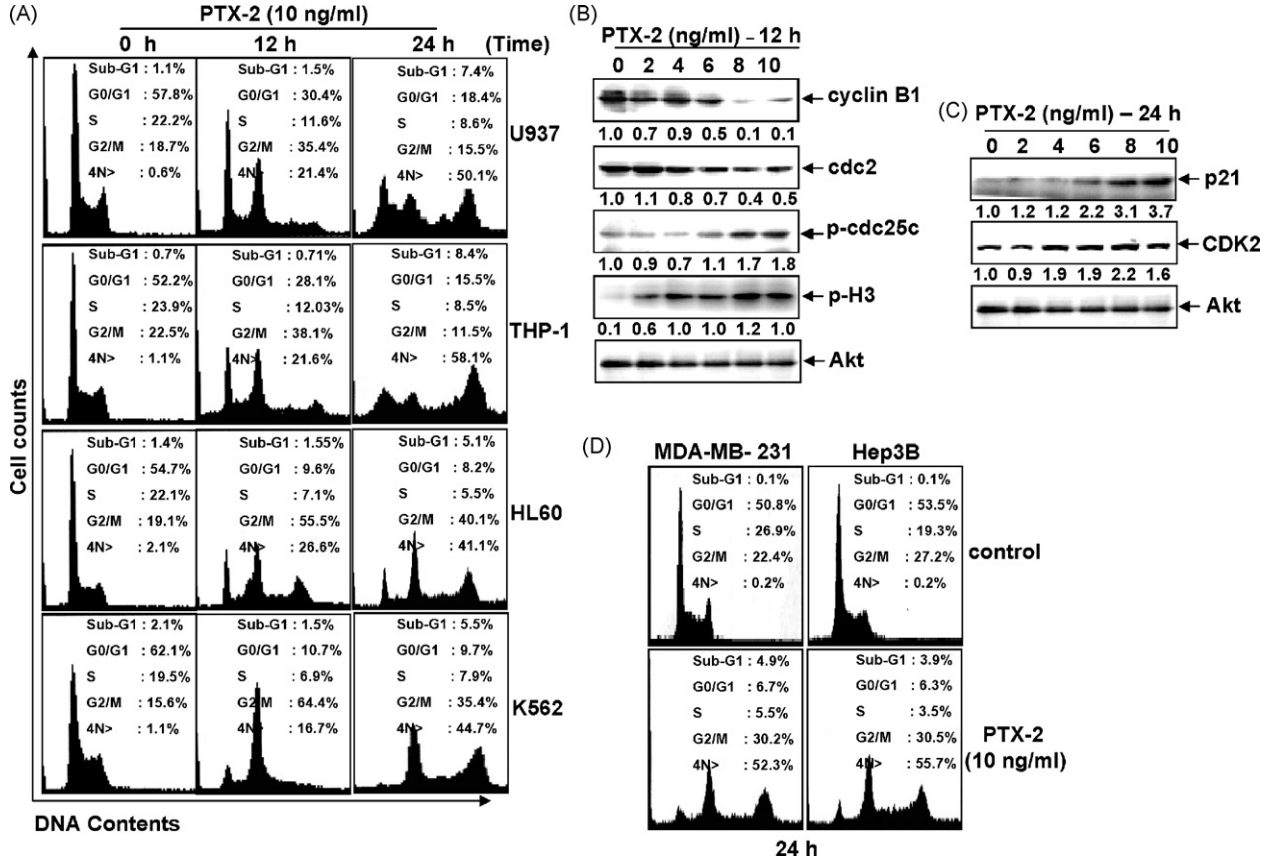

Fig. 4 – Leukemia cells undergo PTX-2–induced G_2/M phase arrest and endoreduplication. Cells were seeded at 5×10^4 cells/ml and were then treated with PTX-2 (10 ng/ml) for the indicated times. (A) Cells were harvested and 10,000 events were analyzed for each sample. DNA content is represented on the *x*-axis and the number of cells counted is represented on the *y*-axis. (B) Cells treated with PTX-2 for 12 h, were lysed for protein extraction. Samples (30 μg protein/lane) were subjected to 12% SDS-PAGE and Western blotting for the detection of specific proteins [anti-cyclin B1, cdc2, p-cdc25c, p-H3]. (C) Cells treated with the indicated concentrations of PTX-2 for 24 h were used for Western blotting, using antibodies against anti-p21 and anti-CDK2. Akt was used as a loading control. (D) MDA-MB-231 and Hep3B were treated with PTX-2 (10 ng/ml) for 24 h. The cells were then analyzed by flow cytometer.

14-3-3. Binding of cdc25c with 14-3-3 induces G_2/M phase arrest *via* ubiquitination [19,20]. Therefore, we examined the effect of PTX-2 on the Ser-216 phosphorylation of cdc25c. As can be seen in Fig. 3B, the level of Ser-216-phosphorylated cdc25c was significantly upregulated by treatment with PTX-2. These results suggest that the PTX-2-induced G_2/M arrest is at least partially due to downregulation of the cyclin B1/cdc2 complexes and phosphorylation of cdc25c. Furthermore, PTX-2 strongly induced phosphorylation of H3, which is a well-known mitosis marker protein (Fig. 4C). A recent study has shown that the increased expression of CDK2 and p21 is associated with endoreduplication [21]. Since CDK2 is an essential component for entry into S phase, consistent or overexpressed CDK2 in G_2/M arrested cells could induce endoreduplication through re-entering S phase. Therefore, we examined the expressions of p21 and CDK2 by Western blotting. As shown in Fig. 4C, the p21 and CDK2 protein levels increased significantly in response to PTX-2. These data suggest that PTX-2 induces G_2/M phase arrest and endoreduplication *via* the modulation of cell cycle-regulating proteins.

3.5. *PTX-2 causes G_2/M arrest and endoreduplication in other human cancer cells*

To test whether the cell types are correlated with their chemosensitivities to PTX-2, we chose two human cancer cell lines (MDA-MB-231 and Hep3B). As shown in Fig. 3D, treatment of PTX-2 (10 ng/ml) for 24 h significantly induced G_2/M phase arrest and endoreduplication in both human cancer cells. PTX-2 also induced an increase in cell size (FSC) and granule content (SSC) in these cells (data not shown). These results indicate that PTX-2 induces G_2/M phase arrest and endoreduplication in other cancer cells.

3.6. *PTX-2 induces ERK- and JNK-dependent cell cycle delay at the G_2/M, as well as endoreduplication*

Because mitogen-activated protein kinase (MAPK) families have also been reported to play an important role in cell cycle transition [22], we evaluated what kinds of MAPKs are involved in PTX-2–induced G_2/M phase arrest and endoreduplication in U937 cells. As shown in Fig. 5A, PTX-2 was found to

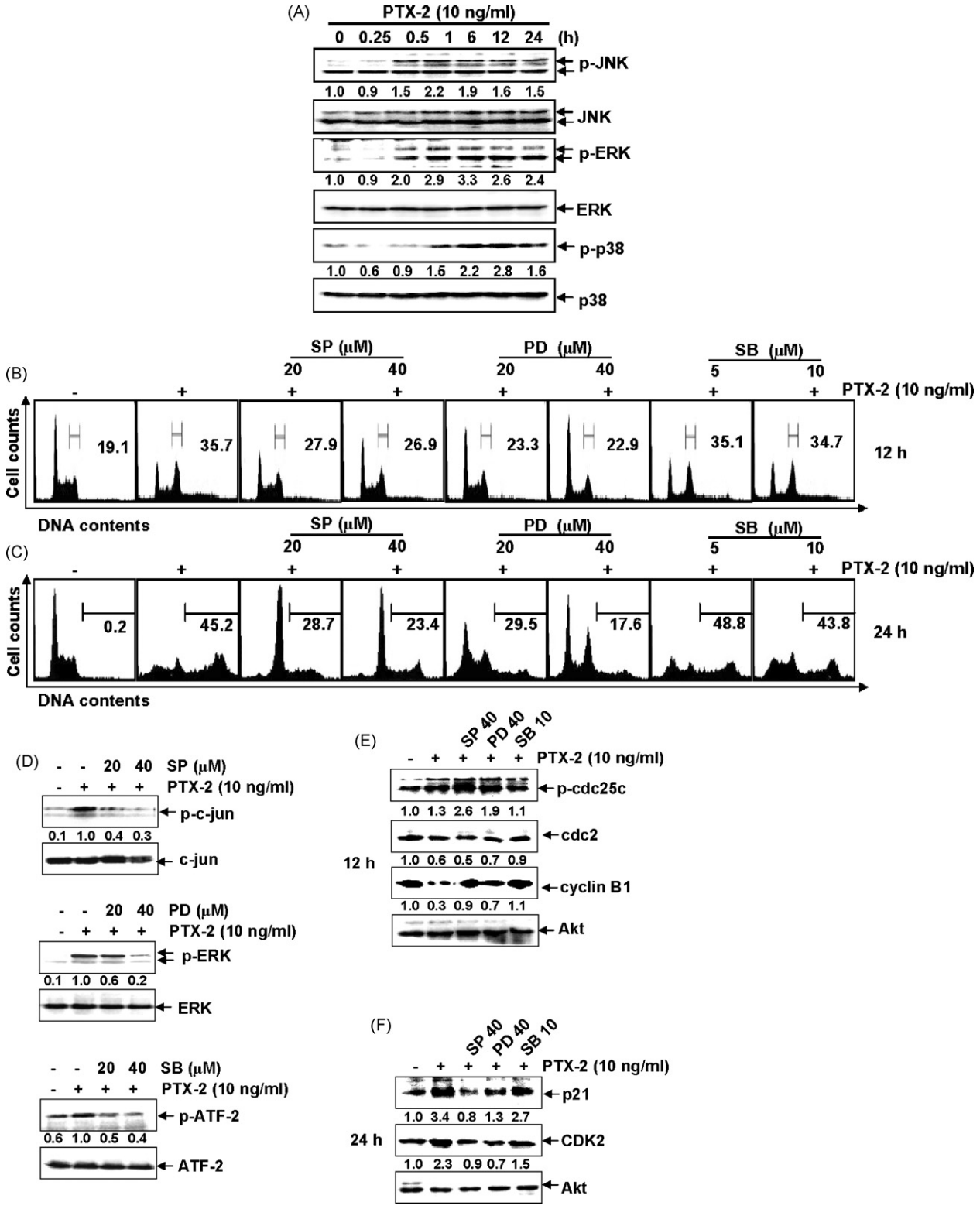

Fig. 5 – PTX-2 induces G_2/M phase arrest and endoreduplication through JNK and ERK activity. (A) U937 cells were treated with PTX-2 (10 ng/ml) for the indicated time. Equal amounts of cell lysates (50 μg) were resolved on SDS-polyacrylamide gels, transferred to nitrocellulose membranes, and probed with antibodies against anti-p-JNK, anti-JNK, anti-p-ERK, anti-ERK, anti-p-p38, and anti-p38. The U937 cells were stimulated with PTX-2 (10 ng/ml) for the indicated time after pretreatment with SP600125 (20 and 40 μM), PD98059 (20 and 40 μM), and SB203580 (5 and 10 μM) for 1 h. The cells were then stained with PI (50 μg/ml) and analyzed by flow cytometry at 12 h (B) and 24 h (C). Portions of the G_2/M (B) and endoreduplication (C) phase are presented. (D) Equal amounts of cell lysates (50 μg) were resolved by SDS-PAGE, transferred to nitrocellulose, and probed with specific antibodies ((D) anti-p-c-jun, anti-c-jun, anti-p-ERK, anti-ERK, anti-p-ATF-2, and anti-ATF-2, (E) p-cdc2, cyclin B1, and cdc2 and (F) p21 and CDK2). Akt was used as internal control. SP, SP600125; PD, PD98059; SB, SB203580.

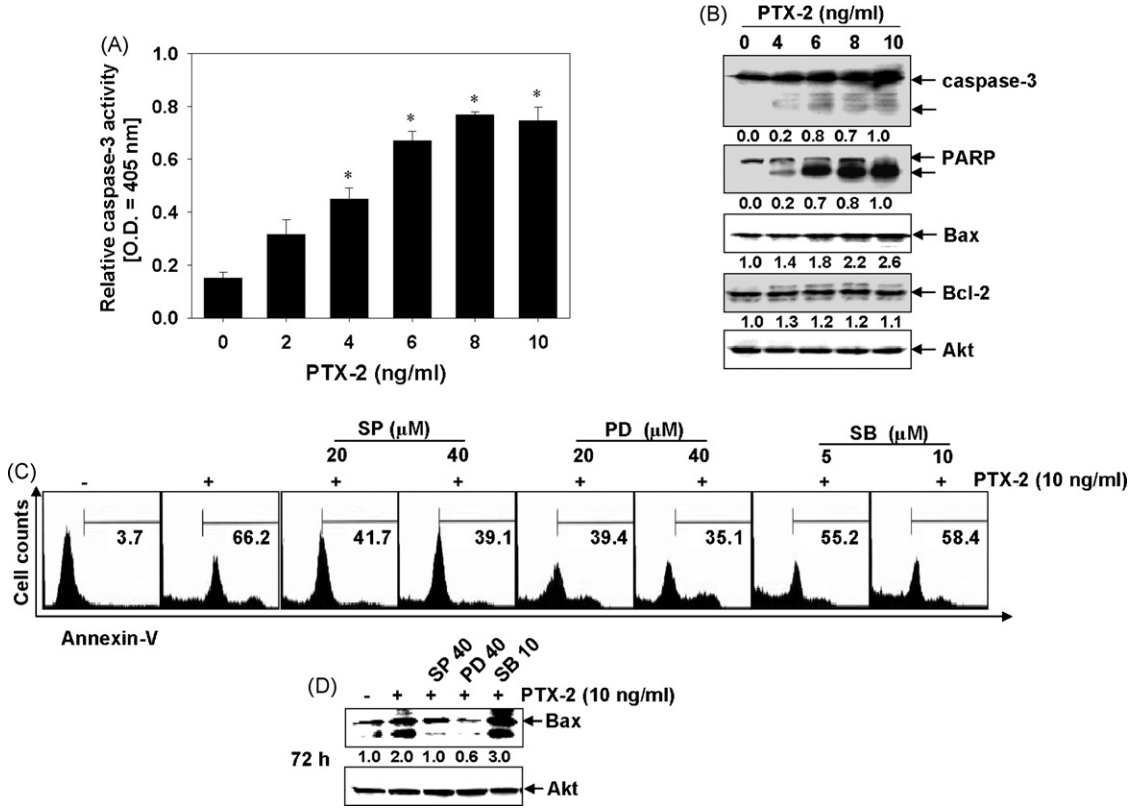

Fig. 6 – PTX-2 induces apoptosis in U937 cells through activation of the ERK and JNK signal pathways. (A) Caspase-3 activity was determined following the manufacturer's protocol. Data are expressed as mean ± S.D. of three independent experiments. (B) Western blots showing the effects of PTX-2 on caspase-3, PARP, Bax, and Bcl-2. U937 cells were stimulated with PTX-2 (10 ng/ml) for 72 h after pretreatment with SP600125 (20 and 40 μM), PD98059 (20 and 40 μM), and SB203580 (5 and 10 μM) for 1 h. (C) The cells were then stained with annexin-V and analyzed by flow cytometer. (D) Equal amounts of cell lysates (50 μg) were resolved by SDS-PAGE, transferred to nitrocellulose, and probed against Bax. Akt was used as internal control. SP, SP600125; PD, PD98059; SB, SB203580.

significantly induce the phosphorylation of ERK, JNK, and p38 from 1 h after PTX-2 treatment. The phosphorylation of MAPKs was sustained to 24 h which is the inducing time of endoreduplication. We next investigated the possible roles of these alterations of MAPK in PTX-2–induced G_2/M cell cycle delay at 12 h. As shown by flow cytometry analysis (Fig. 5B), pretreatment with 40 μM PD98059 (an inhibitor of ERK) and 40 μM SP600125 (an inhibitor of JNK) resulted in a greater decrease of the G_2/M cell population (28 ± 3% and 22 ± 2%) in U937 cells than when treated with PTX-2 alone (36 ± 5%). PTX-2–induced endoreduplication (45 ± 4%) at 24 h was also significantly and statistically decreased by pretreatment with 40 μM PD98059 (17 ± 3%) and 40 μM SP600125 (23 ± 3%) (Fig. 5C). However, SB203580 (an inhibitor of p38) did not affect the PTX-2-induced cell cycle and endoreduplication alterations. In order to confirm that this effect was specific for the MAPK pathway, the phosphorylation states of c-jun (a downstream of JNK), ERK, and ATF-2 (a downstream of p38), were assessed by Western blot analysis at 24 h. As shown in Fig. 5D, the phosphorylation was significantly attenuated by treatment with MAPK inhibitors. These results indicate that the ERK and JNK signaling pathways are involved in PTX-2-induced actin dysfunction, suggesting the presence of an actin checkpoint at the G_2/M transition in leukemia cells.

Next, we examined whether inhibitors of MAPKs modulate protein expression in PTX-2-induced G_2/M phase and endoreduplication. As can see in Fig. 5E and F, SP600125 and PD98059 more increased p-cdc25c expression induced by PTX-2 treatment at 12 h, but p21 and CDK2 was significantly downregulated at 24 h. Interestingly, powerful expression of p-cdc25c by these two inhibitors significantly increased G_2/M phase arrest at 24 h to block endoreduplication. These data suggest that JNK and ERK is associated with delay of PTX-2-induced G2/M phase arrest and endoreduplication.

3.7. *PTX-2 induces apoptosis through the ERK and JNK signal pathways*

To assess whether apoptosis contributes to the growth inhibitory effects of PTX-2, we assayed the effects of PTX-2 on apoptosis in U937 cells. As shown in Fig. 6A, PTX-2 exposure predominantly increased caspase-3 activity in a dose-dependent manner. As shown by the Western blot analysis in Fig. 6B, PTX-2 also resulted in the induction of a cleaved form of capases-3 in a dose-dependent manner. The induction of apoptosis was additionally confirmed by the cleavage of PARP. Because Chae et al. [11] have shown that Bcl-2 families are involved in PTX-2-induced apoptosis, we analyzed the

expression of Bcl-2 and Bax. As shown in Fig. 6B, PTX-2 treatment induced upregulation of Bax, but did not show any effect on Bcl-2 expression.

To evaluate what kinds of MAPKs are involved in PTX-2–induced apoptosis in U937 cells, annexin-V staining was conducted. As shown by flow cytometry analysis (Fig. 6C), pretreatment of SB203580 did not affect PTX-2–induced apoptosis ($58 \pm 4\%$) as compared with PTX-2 treatment ($66 \pm 5\%$), while treatment with 40 μM SP600125 and 40 μM PD98059 significantly attenuated the PTX-2–induced annexin-V positive cell population at $38 \pm 3\%$ and $34 \pm 4\%$, respectively. These two inhibitors, but not SB203580 also more decreased Bax expression in PTX-2-treated cells at 72 h (Fig. 6D). These results indicate that PTX-2-induced apoptosis is mainly mediated through the activation of the JNK and ERK signal pathways, but not the p38 signal pathway.

4. Discussion

PTX-2 is suspected to be the precursor from which many PTXs are derived through biotransformation, and has anticancer effects [11]. However, the precise mechanism of PTX-2-mediated cell growth inhibition is fully unknown. In the present study, we found that PTX-2 causes G_2/M phase arrest and apoptosis in human cancer cell lines. Furthermore, multinucleation, which is one of the characteristic features of the cytokinesis inhibition, was observed in the presence of PTX-2. These results provide the first evidence that PTX-2 induces abnormal cell cycle transition through the disruption of actin dynamics.

The mitosis phase in normal human cells is initiated by the cdc2/cyclin B1 complex through regulation of cdc25c, however in cancer cells, these proteins are deregulated, so that normal growth control and checkpoints are evaded [23,24]. Increased cdc25c phosphatase activity could lead to the activation of cdc2/cyclin B, which results from the dephosphorylation of cdc2 by cdc25c [25]. In contrast, phosphorylation of cdc25c on Ser-216 decreases its phosphatase activity through the cytoplasmic translocation of cdc25c with 14-3-3 from the nucleus. This is known to be an important regulatory protein inducing delay or blocking mitotic entry [26]. In this study, we found that PTX-2-induced G_2/M phase arrest is associated with the repression of cdc2 and cyclin B1 expression, and induction of the phosphorylation of cdc25c at Ser-216. Additionally, the elevated expression of CDK2 and p21 could induce traversal to the S phase from the mitotic phase, hence, the cells undergo endoreduplication [21]. The proteins can downregulate the cdc2 and cyclin B1 complex to induce G_2/M phase arrest. These results may imply that exposure to PTX-2 induces G_2/M phase arrest and endoreduplication through the downregulation of the cdc2/cyclin B1 complex *via* the phosphorylation of cdc25c and the evaluation of p21 expression.

Recent studies have importantly reported that the ERK and the JNK signal pathways regulate G_2/M phase arrest and endoreduplication through cdc2/cyclin B1 complex *via* the inactivation and phosphorylation of cdc25c [27,28]. Actin dysfunction also accelerates the ERK and the JNK signal pathways, and delays entry into mitosis in mammalian cells [29,30]. Above reports indicate that these two MAPKs are closely involved in actin depolymerization or polymerization on G_2/M phase arrest and endoreduplication. MAPK cascades have been also shown to play a key role in proliferation, differentiation, development, transformation, and apoptosis [22]. Therefore, we determined the functional relationship between MAPK activity and G_2/M phase arrest, endoreduplication, and apoptosis in the presence of PTX-2, and thus determined that ERK and JNK, but not p38, delayed PTX-2–induced G_2/M phase arrest, endoreduplication, and apoptosis.

The function of microtubules, another cytoskeletal components, has been frequently studied in the G_2/M cell cycle phase. For example, treatment with microtubulin-interfering agents, such as nocodazole and taxol, induces tetraploidy arrest because sister chromatid segregation is interrupted [31]. This mitotic failure state could result in an excessive endoreduplication by prolonged exposure to microtubule-interfering agents. Additionally, Topo II inhibitors such as etoposide, amsacrine, and merbarone can induce endoreduplication by preventing the decatenation of replicated chromosomes, which subsequently fail to complete normal segregation at mitosis [32,33]. Our observations revealed that PTX-2 slightly increases Topo II phosphorylation and activity. However, we confirmed that microtubulin polymerization and Topo II are not involved in cytokinesis by PTX-2. Nevertheless, further studies are necessary to determine why Topo II phosphorylation in the nucleus is increased in PTX-2-induced endoreduplication.

Here, we provide the first assessment of the mechanism whereby PTX-2 induces cell cycle-dysfunction and cell death in leukemia cells. We demonstrated that PTX-2 arrests proliferating leukemia cells in the G_2/M phase, and induces endoreduplication and apoptosis through phosphorylation of the ERK and JNK signal pathways. PTX-2 also has strong anticancer effects against leukemia cells and it also causes a dose-dependent increase in G-actin, promotes actin depolymerization, and disrupts the organization of the actin cytoskeleton.

Acknowledgment

This work was supported by Korea Sea Grant Program (Honam Sea Grant) from Ministry of Maritime Affairs & Fisheries, South Korea.

REFERENCES

[1] Schoenenberger CA, Bischler N, Fahrenkrog B, Aebi U. Actin's propensity for dynamic filament patterning. Fed Eur Biochem Soc Lett 2002;529:27–33.
[2] Robinson DN, Spudich JA. Towards a molecular understanding of cytokinesis. Trends Cell Biol 2000;10:228–37.
[3] Pollard TD, Borisy GG. Cellular motility driven by assembly and disassembly of actin filaments. Cell 2003;112:453–65.
[4] Carlier MF, Ressad F, Pantaloni D. Control of actin dynamics in cell motility. Role of ADF/cofilin. J Biol Chem 1999;274:33827–30.
[5] Senderowicz AM, Kaur G, Sainz E, Laing C, Inman WD, Rodriguez J, et al. Jasplakinolide's inhibition of the growth

of prostate carcinoma cells in vitro with disruption of the actin cytoskeleton. J Natl Cancer Inst 1995;87:46–51.
[6] Udagawa T, Yuan J, Panigrahy D, Chang YH, Shah J, D'Amato RJ, et al. an epoxide containing *Aspergillus* derived fungal metabolite, inhibits angiogenesis and tumor growth. J Pharmacol Exp Ther 2000;294:421–7.
[7] Saito S, Watabe S, Ozaki H, Fusetani N, Karaki H, Mycalolide B. a novel actin depolymerizing agent. J Biol Chem 1994;269:29710–4.
[8] Nakatani K, Murayama T, Satoh Y, Furukawa K, Omura S, Ohizumi Y. Modulation of actomyosin ATPase by thiotetromycin is mediated through conformational change of actin. Eur J Pharmacol 1999;383:381–6.
[9] Draisci R, Lucentini L, Mascioni A. In: Botana LM, editor. Seafood and Freshwater Toxins: Pharmacology, Physiology, and Detection. New York: Marcel Dekker, Inc.; 2000. p. 289–324.
[10] Yasumoto T, Murata M, Oshima Y, Sano M, Matsumoto GK, Clardy J. Diarrheic shellfish toxins. Tetrahedron 1985;41:1019–25.
[11] Chae HD, Choi TS, Kim BM, Jung JH, Bang YJ, Shin DY. Oocyte-based screening of cytokinesis inhibitors and identification of pectenotoxin-2 that induces Bim/Bax-mediated apoptosis in p53-deficient tumors. Oncogene 2005;24:4813–9.
[12] Hori M, Matsuura Y, Yoshimoto R, Ozaki H, Yasumoto T, Karaki H. Actin depolymerizing action by marine toxin, pectenotoxin-2. Nippon Yakurigaku Zasshi 1999;114: 225P–9P.
[13] Saito S, Karaki H. A family of novel actin-inhibiting marine toxins. Clin Exp Pharmacol Physiol 1996;23:743–6.
[14] Jung JH, Sim CJ, Lee CO. Cytotoxic compounds from a two-sponge association. J Nat Prod 1995;58:1722–6.
[15] Huang ZJ, Haugland RP, You WM, Haugland RP. Phallotoxin and actin binding assay by fluorescence enhancement. Anal Biochem 1992;200:199–204.
[16] Isaacs RJ, Davies SL, Sandri MI, Redwood C, Wells NJ, Hickson ID. Physiological regulation of eukaryotic topoisomerase II. Biochim Biophys Acta 1998;1400:121–37.
[17] Cantero G, Pastor N, Mateos S, Campanella C, Cortes F. Cisplatin-induced endoreduplication in CHO cells: DNA damage and inhibition of topoisomerase II. Mutat Res 2006;599:160–6.
[18] Mateos S, Dominguez I, Pastor N, Cantero G, Cortes F. The DNA demethylating 5-azaC induces endoreduplication in cultured Chinese hamster cells. Mutat Res 2005;578:33–42.
[19] Muslin AJ, Xing H. 14-3-3 proteins: regulation of subcellular localization by molecular interference. Cell Signal 2000;12:703–9.
[20] Mackintosh C. Dynamic interactions between 14-3-3 proteins and phosphoproteins regulate diverse cellular processes. Biochem J 2004;381:329–42.
[21] Chang BD, Broude EV, Fang J, Kalinichenko TV, Abdryashitov R, Poole JC, et al. $p21^{Waf1/Cip1/Sdi1}$-induced growth arrest is associated with depletion of mitosis-control proteins and leads to abnormal mitosis and endoreduplication in recovering cells. Oncogene 2000;19:2165–70.
[22] Zhang W, Liu HT. MAPK signal pathways in the regulation of cell proliferation in mammalian cells. Cell Res 2002;12: 9–18.
[23] Jin P, Hardy S, Morgan DO. Nuclear localization of cyclin B1 controls mitotic entry after DNA damage. J Cell Biol 1998;141:875–85.
[24] Evan GI, Vousden KH. Proliferation, cell cycle and apoptosis in cancer. Nature 2001;411:342–8.
[25] Sanchez Y, Wong C, Thoma RS, Richman R, Wu Z, Piwnica-Worms H, et al. Conservation of the Chk1 checkpoint pathway in mammals: linkage of DNA damage to Cdk regulation through Cdc25. Science 1997;277:1497–501.
[26] Peng CY, Graves PR, Thoma RS, Wu Z, Shaw AS, Piwnica-Worms H. Mitotic and G_2 checkpoint control: regulation of 14-3-3 protein binding by phosphorylation of Cdc25C on serine-216. Science 1997;277:1501–5.
[27] Wang R, He G, Nelman-Gonzalez M, Ashorn CL, Gallick GE, Stukenberg PT, et al. Regulation of Cdc25C by ERK-MAP kinases during the G_2/M transition. Cell 2007;128:1119–32.
[28] Goss VL, Cross JV, Ma K, Qian Y, Mola PW, Templeton DJ. SAPK/JNK regulates cdc2/cyclin B kinase through phosphorylation and inhibition of cdc25c. Cell Signal 2003;15:709–18.
[29] Reiterer G, Yen A. Inhibition of the janus kinase family increases extracellular signal-regulated kinase 1/2 phosphorylation and causes endoreduplication. Cancer Res 2006;66:9083–9.
[30] Lee K, Song K. Actin dysfunction activates ERK1/2 and delays entry into mitosis in mammalian cells. Cell Cycle 2007;6:1487–95.
[31] Jordan MA, Toso RJ, Thrower D, Wilson L. Mechanism of mitotic block and inhibition of cell proliferation by taxol at low concentrations. Proc Natl Acad Sci USA 1993;90:9552–6.
[32] Sumner AT. Induction of diplochromosomes in mammalian cells by inhibitors of topoisomerase II. Chromosoma 1998;107:486–90.
[33] Drake FH, Hofmann GA, Mong SM, Bartus JO, Hertzberg RP, Johnson RK, et al. *In vitro* and intracellular inhibition of topoisomerase II by the antitumor agent merbarone. Cancer Res 1989;49:2578–83.